

IRRADIATION CREEP OF CHEMICALLY VAPOR DEPOSITED SILICON CARBIDE AS ESTIMATED BY BEND STRESS RELAXATION METHOD—Y. Katoh, L. L. Snead, S. Kondo (Oak Ridge National Laboratory), T. Hinoki, A. Kohyama (Kyoto University)

OBJECTIVE

The objective of this work was to develop a technique to experimentally determine the neutron irradiation-induced creep deformation behavior of brittle bulk ceramics and fibrous ceramic composites, and to study the irradiation creep of chemically vapor-deposited silicon carbide and uni-directionally reinforced silicon carbide fiber, chemically vapor-infiltrated silicon carbide matrix composites. The initial experimental result is discussed in this report.

SUMMARY

Bend stress relaxation technique was successfully applied for the study on irradiation creep of chemically vapor-deposited beta-phase silicon carbide (SiC) ceramics and vapor-infiltrated composites. Samples machined into thin strips were held within a curved gap in the silicon carbide fixture, and irradiated in High Flux Isotope Reactor at Oak Ridge National Laboratory and Japan Materials Test Reactor at Japan Atomic Energy Agency to the maximum neutron fluences of 0.74×10^{25} n/m² ($E > 0.1$ MeV) at 400–1030°C. Irradiation creep strain for SiC exhibited weak temperature dependence in the temperature range studied. The creep strain appeared highly non-linear to neutron fluence due to the early domination of the initial transient irradiation creep. The transient creep was speculated to have caused by the rapid development of defect clusters and the structural relaxation of as-grown defects during early stages of irradiation damage accumulation. Steady-state irradiation creep compliance of SiC was conservatively estimated to be $2\text{--}3 \times 10^{-32}$ (MPa-n/m²)⁻¹ at ~600–~1,100°C. The observed smaller irradiation creep strains for the monocrystalline SiC and the uni-directional composites than for the polycrystalline SiC were attributed to differences in the transient creep strain.

PROGRESS AND STATUS

Introduction

Silicon carbide (SiC) and composite materials of SiC are among the key engineering materials for nuclear applications including fusion and advanced fission energy and nuclear propulsion systems [1–3]. The promises and attractiveness of SiC ceramics rely on their unique combined properties such as neutron irradiation resistance, high temperature strength and inertness, low electrical conductivity, low activation / low decay heat, low tritium permeability, and low specific mass. Recent advancement of SiC-based ceramic composite technology has triggered the efforts toward practical applications of continuous SiC fiber-reinforced SiC-matrix ceramic composites (SiC/SiC composites) to the fusion blanket structural and multi-functional components [1,4] and the gas-cooled fission reactor core components [5,6].

One of the most critical issues which have not yet been addressed for SiC ceramics and composites for nuclear structural applications is irradiation creep [7]. Irradiation creep is the anisotropic plastic deformation driven by external or internal stresses, and induced or enhanced by irradiation in excess of thermal creep deformation. Irradiation creep generally dominates creep deformation of irradiated materials

Table 1. List of materials irradiated in this work.

Material	Crystal Structure	Manufacturer	Density (g/cm ³)	Purity (%)		
CVD SiC	Polycrystalline beta	Rohm & Haas	3.21	>99.9995		
3C SiC	Monocrystalline beta	Hoya	3.21	~99.99 ¹⁾		
Material	Fiber / Architecture	Interphase	Matrix	V _f ²⁾ (%)	Density (g/cm ³)	Porosity (%)
UD-TySA/PyC ³⁾	Tyranno™-SA	PyC ^{520nm}	SiC ^{CVI}	~30	~2.6	~17
UD-TySA/ML ⁴⁾	Uni-directional	5x(PyC ^{20nm} /SiC ^{100nm})				

¹⁾ Doped nitrogen as major impurity. ²⁾ Fiber volume fraction. ³⁾ Pyrolytic carbon interphase ⁴⁾ Multilayered interphase.

at temperatures below thermal creep practically operates for conventional metals and alloys.

Studies on irradiation creep of SiC (-based materials) are so far very limited. Irradiation creep of chemically vapor-deposited SiC has been studied by Price in 1977 [8]. In that work, elastically bent strip samples of chemically vapor-deposited (CVD) SiC were irradiated in a fission reactor, and the creep compliance was estimated to be $\sim 1 \times 10^{-6} \text{ MPa}^{-1} \text{ dpa}^{-1}$ at 780–1130°C. Scholz and co-workers [9–12] measured the creep deformation of SCS-6 CVD SiC-based fiber, which was torsionally loaded under penetrating proton or deuteron beam irradiation. They reported several important observations including the linear stress and flux dependency of the tangential creep rate at 600°C, and an approximate irradiation creep compliance of $\sim 1 \times 10^{-5} \text{ MPa}^{-1} \text{ dpa}^{-1}$, which is only weakly and non-monotonically dependent on irradiation temperature in 450–1,100°C range. The adopted experimental method and setup in this work are reliable. However, the determined irradiation creep compliances are more than an order larger than those reported for neutron irradiation by Price [8]. Moreover, the CVD SiC fiber used is known to exhibit anomalous thermal creep behavior presumably due to excess silicon on grain boundaries [13].

For high purity, stoichiometric, vapor-deposited SiC, which is relevant to SiC ceramics and SiC/SiC composites' constituents considered for nuclear applications, there have not been convincing neutron irradiation creep compliance data available. The present work is intended to help understanding the creep behavior of such materials under neutron irradiation at elevated temperatures. An experimental method utilizing the technique of bend stress relaxation was employed. This paper describes the experimental method adopted, reports the initial results, and discusses their implication.

Experimental Procedures

The bend stress relaxation (BSR) technique was adopted by Morscher and DiCarlo for evaluation of thermal creep behavior of ceramic fibers [14]. In a BSR irradiation creep experiment, samples in a form of straight thin fiber or strip are constrained to the bend radius R_0 at temperature T and damage rate ϕ for a period t . The bend stress retention ratio (BSR ratio, m) is defined by

$$m(\phi, T, t) = \frac{\sigma_a}{\sigma_0} = 1 - \frac{R_0}{R_a} \quad (1)$$

where σ_a and σ_0 are the initial and the final bend stresses, respectively, and R_a is the unconstrained bend radius after heat treatment, assuming a constant elastic modulus. When a linear stress dependence of steady-state irradiation creep rate $\dot{\epsilon}_{ic}$ is assumed,

$$\dot{\epsilon}_{ic} = \kappa \sigma \phi \quad (2)$$

the irradiation creep compliance κ can be derived by the following equation,

$$\kappa = \frac{\ln(m_1/m_2)}{E\phi(t_2 - t_1)} \quad (3)$$

using m values at two different dose levels.

Compared to the conventional experimental techniques for irradiation creep studies such as the pressurized tube creep and externally loaded in-pile tensile or compressive creep techniques, BSR technique requires only very small specimens in a simple geometry. However, the successful application of BSR technique to irradiation creep study of bulk ceramics hinges upon preparation of thin strip samples with sufficient flexural strength and the appropriate design of specimen holders that ensure the thermal contact with the specimens without imposing undesired interactions.

For the first set of experiment, thin strip samples with dimensions of 25 or 40 mm x 1 mm x 50 μm were prepared. Materials used were high purity (>99.9995%) beta-phase (3C) CVD SiC manufactured by Rohm and Haas Co., Advanced Materials (Waborn, Massachusetts, USA), and a free-standing monocrystalline

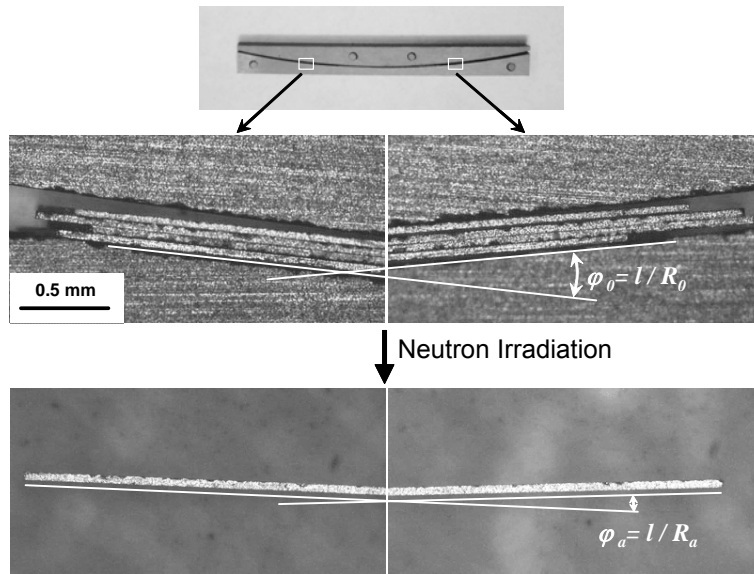


Fig. 1. Appearance of assembled BSR irradiation creep holder (top) and magnified views of end sections of thin strip specimens before (middle) and after (bottom) creep deformation.

Table 2. Summary of irradiation condition and result of BSR irradiation creep experiment.

Material	T _{irr} °C	Fluence x10 ²⁵ n/m ²	Reactor	Initial / final bend stress MPa	Initial / final bend strain x10 ⁻⁴	Creep strain x10 ⁻⁴	BSR ratio <i>m</i>	Average creep compliance x10 ⁻³⁷ (Pa-n/m ²) ⁻¹
CVD SiC	400	0.6	JMTR	82 / 60	1.80 / 1.39	0.41	0.77	0.97
	600	0.2	JMTR	81 / 57	1.80 / 1.31	0.49	0.73	3.5
		0.6	JMTR	81 / 46	1.80 / 1.05	0.75	0.58	2.0
	700*	0.66	HFIR	58 / 45**	1.52 / 1.04**	0.48**	0.69	1.3**
	750	0.6	JMTR	80 / 55	1.80 / 1.27	0.53	0.71	1.3
	1030*	0.74	HFIR	86 / 53**	1.94 / 1.23**	0.71**	0.63	1.4**
3C SiC	700*	0.66	HFIR	68 / 58**	1.52 / 1.32**	0.20**	0.87	0.47**
	1030*	0.74	HFIR	86 / 74**	1.94 / 1.22**	0.72**	0.88	0.40**
UD-TySA/PyC	600	0.2	JMTR	59 / 48	1.80 / 1.50	0.30	0.83	2.8
UD-TySA/ML	600	0.2	JMTR	63 / 55	1.80 / 1.62	0.18	0.90	1.5

*Calculated temperature. **Rough measurement; to be updated.

wafer of 3C-SiC with {100} surface orientation provided by Hoya Advanced Semiconductors Technologies, Inc. (Tokyo, Japan). The monocrystalline specimens were machined so that the longitudinal direction is in parallel with one of the <011> orientations. The specimens, after the finish-grinding with diamond paste, exhibited typical flexural strength of ~400 MPa, which enables the minimum bending radius of ~30 mm. In addition to the monolithic CVD SiC materials, small number of uni-directionally reinforced Tyranno™-SA fiber, chemically vapor-infiltrated SiC matrix composites were included to the materials to be evaluated. The SiC ceramics and composites tested are summarized in [Table 1](#).

The specimen holder was designed to retain the thin strip samples in a narrow gap with a curvature of 100mm radius. The appearance of the assembled specimen holder and the procedure to measure the constrained and the unconstrained specimen curvatures are shown in [Fig. 1](#). CVD SiC and Hexoloy™ SA were used as the holder materials in order to avoid potential chemical interactions with the SiC specimens during irradiation. The bend radii were determined by measuring the differential tangential angles at both ends of the sample strips before (constrained) and after (unconstrained) irradiation, as shown in Fig. 1. The accuracy of bend angle measurement by optical microscopy was <0.1°, which gives <1% error in determination of the BSR ratios.

The irradiation was performed at High Flux Isotope Reactor (HFIR), Oak Ridge National Laboratory (Oak Ridge, Tennessee, USA), and Japan Materials Test Reactor (JMTR), Japan Atomic Energy Agency (Oarai, Japan) to the maximum neutron fluence of 7.4x10²⁴ n/m² (E>0.1 MeV, the same shall apply hereinafter). The nominal irradiation temperatures were 700 and 1,030°C for HFIR, and 400, 600, and 750°C for JMTR. Details of the irradiation conditions are summarized in [Table 2](#).

Results

The result of strain measurement is summarized in Table 2. The strain and stress values are the maximum that occurs at the tensile and compressive surfaces of bent specimens. The creep strain corresponds to the unconstrained residual strain, and the final bend strain was determined by subtracting the creep strain from the initial elastic strain. The initial and the final bend stresses were determined using temperature-dependent Young's modulus data for non-irradiated CVD SiC [15]. The linear-averaged irradiation creep compliances, $\bar{\kappa}$, were derived by dividing the creep strain by the product of fluence and the linear-averaged stress.

Neutron irradiation is known to lower Young's modulus of CVD SiC by a few to several percent at the temperatures for this experiment [16]. Such change in Young's modulus occurs mostly before a few dpa of irradiation damage is achieved. Since the irradiation effect on elastic modulus was neglected here, the $\bar{\kappa}$ data may involve a few percent errors due to this.

In Fig. 2, the irradiation-creep BSR ratios are plotted as a function of irradiation temperature for the polycrystalline ('CVD SiC') and monocrystalline ('3C SiC') materials. The obvious features are: 1) the general lack of temperature dependence, 2) the distinctively smaller creep deformation for the monocrystalline samples, and 3) a reasonable agreement between data from HFIR and JMTR. A slightly negative correlation between the BSR ratio and irradiation temperature could be noticed, but the temperature effect does not appear significant compared to the error bars shown. The error bars correspond to the ranges of scatter for the data from JMTR, whereas they represent the maximum cumulative uncertainty associated with the bend radius measurement for the data from HFIR.

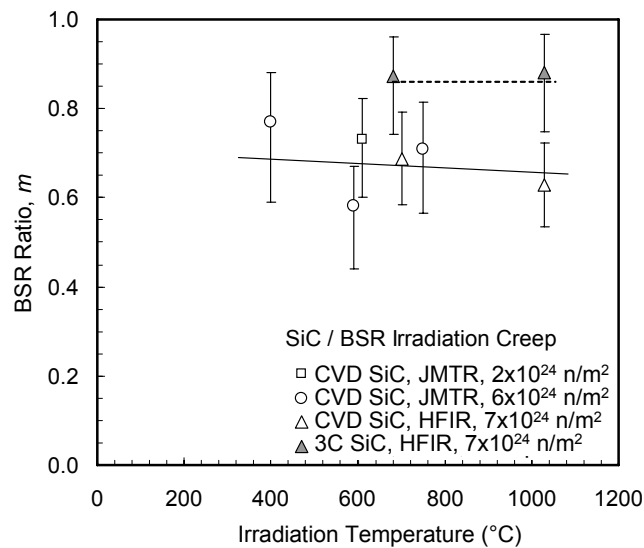


Fig. 2. Bend stress retention ratios for the irradiated polycrystalline ('CVD SiC') and monocrystalline ('3C SiC') vapor-deposited beta-phase SiC, as a function of irradiation temperature.

Discussion

The linear-averaged irradiation creep compliance values, $\bar{\kappa}$, in Table 2, which have been obtained by putting $t_l = 0$ and $m_l = 1$ in Eq. 3, are obviously not appropriate for predicting the long-range irradiation creep behavior of SiC. For the light ion-irradiated SCS-6 fiber, Scholz et al. reports domination of the primary transient creep until at least 0.05 dpa, potentially followed by a transition into the steady-state-like creep, at 600°C [12]. They attributed the primary creep behavior to anisotropic partitioning of excess vacancies in association with the rapid interstitial cluster formation during the initial phase of irradiation process in SiC, by correlating the transient creep rate with the swelling rate of SiC at the relevant temperatures [12]. The fluence dependence of the BSR ratio observed at 600°C in this work supports the early domination of transient irradiation creep. Meanwhile, Eq. 2 also assumes the linear dependence of irradiation creep rate on the stress magnitude and neutron flux. The assumptions of linear stress and flux dependence may be adequate because of the light-ion data reported by Scholz et al. [9] but will have to be confirmed by neutron irradiation in future work.

Fig. 3 presents the irradiation creep BSR ratios obtained from this work and calculated from data published by Price [8], as a function of neutron fluence. Those data do not indicate constant creep compliance but represent a rather steep stress relaxation before a fluence of $0.2 \times 10^{25} \text{ n/m}^2$ is achieved and the domination of that initial relaxation to the total stress relaxation at $\sim 0.6 \times 10^{25} \text{ n/m}^2$. It is not clear if the fluence of $\sim 0.6 \times 10^{25} \text{ n/m}^2$ is still within the transient creep regime or not. However, at 600–750°C, the BSR ratios similar to that at $0.2 \times 10^{25} \text{ n/m}^2$ suggest that it is close to the end of the transient creep regime at $\sim 0.6 \times 10^{25} \text{ n/m}^2$. The near-saturation of swelling at <1 dpa in this temperature range [17] also supports this implication, assuming the correlation of irradiation creep and low temperature swelling proposed by Scholz [12].

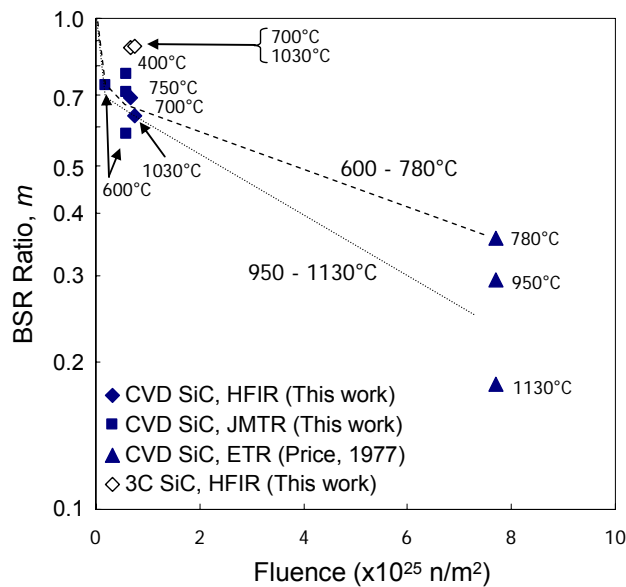


Fig. 3. Neutron fluence dependence of irradiation creep BSR ratio. Note that slope is proportional to irradiation creep compliance.

In ion-irradiated CVD SiC, Kondo et al. found that the number density of Frank faulted loops of interstitial type is strongly dependent on the relative orientation to the surface [18]. In their observation, loops on a {111} family plane that was near parallel to the free surface were abundantly present, whereas those on planes near perpendicular to the surface were notably rare. Because of the shallow damage range ($\sim 2 \mu\text{m}$) in their ion irradiated sample, significant lateral compressive stress develops by swelling during the early irradiation. Therefore, the observation implies that the nucleation of interstitial loops was allowed only in orientations which do not cause expansion to the compressively stressed directions. Anisotropic swelling and/or creep by the mechanism of stress-induced preferred nucleation (SIPN) of dislocation loops was concluded in that work. Although this observation was at $1,400^\circ\text{C}$, it may be possible that a similar mechanism operates at lower temperatures for present work, since dislocation loop-like interstitial clusters develop even at below 800°C and low doses [19]. Assuming that the rapid production of aligned interstitial clusters are contributors to the initial transient creep, it is reasonable to expect the regime of steady-state(-like) creep follows through the growth and progressive nucleation of those clusters.

Based on the discussion above, it is possible that a steady-state irradiation creep is almost achieved at $\sim 0.6 \times 10^{25} \text{ n/m}^2$. Under such an assumption, steady-state creep compliances of $\sim 2 \times 10^{-32}$ and $\sim 3 \times 10^{-32} (\text{MPa}\cdot\text{n/m}^2)^{-1}$ at $600\text{--}780^\circ\text{C}$ and $950\text{--}1,030^\circ\text{C}$, respectively, can be derived from data shown in Fig. 3. They are plotted in Fig. 4, along with the linear-averaged irradiation creep compliance values from the present work and by Price [8], and the light-ion creep compliance values published by Scholz [12]. Fig. 4 clearly depicts that the linear-averaged compliance values are strongly affected by the transient creep component. For the same reason, the steady-state creep compliance determined upon the relaxation

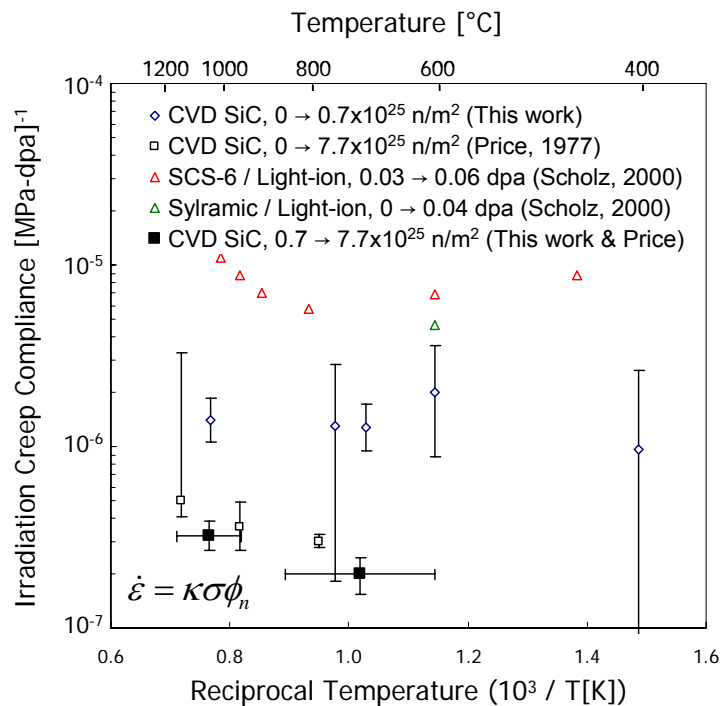


Fig. 4. Irradiation creep compliance of chemically vapor deposited SiC and SiC-based materials estimated by various experiments.

behavior between ~ 0.6 and 7.7×10^{25} n/m² may still be a conservative estimation. The very large compliance values for the light ion irradiation creep are primarily due to the fact that they represent tangent compliances at a certain dose within the transient creep regime, while the presumably higher defect production efficiency by light ions and the non-stoichiometric grain boundary chemistry might have contributed as well.

The observed difference in stress relaxation behavior between the polycrystalline and monocrystalline materials is notable. The possible explanations include: 1) crystallographic orientation effect and 2) the influence of as-grown defects including grain boundaries. Assuming {111} as the primary habit planes for the responsible microstructural defects, in the monocrystalline specimens, two planes are in parallel and the other planes are $\sim 53^\circ$ inclined to the stress axis. On the other hand, in the polycrystalline specimens, one of the {111} planes is in parallel and three others are $0\text{--}71^\circ$ inclined to the stress axis. Hence, significant crystallographic orientation effect is not anticipated in this situation. As to the effect of as-grown defects, the polycrystalline material contains grain and subgrain boundaries and stacking faults, twin boundaries, and dislocations, whereas only the very low density stacking faults have been observed in the monocrystalline material [20]. It's been speculated that the thermally activated relaxation of these defects are partly responsible for the primary thermal creep deformation of stoichiometric SiC [21]. The primary thermal creep strain in CVD SiC is known to reach as high as $>1 \times 10^{-4}$ at 1500°C , and it is reasonable to assume that a similar deformation mechanism can operate at significantly lower temperatures in assist of irradiation. Therefore, the effect of as-grown defects is more likely than the effect of crystallographic orientation as the reason for the different irradiation creep strains at a low dose.

It is also interesting to note the significantly smaller fractional stress relaxation for the uni-directional composites than for polycrystalline monolithic SiC. Since the composites consists primarily of beta-phase polycrystalline SiC, and the pyrolytic carbon interphase itself should exhibit much larger irradiation creep compliance than SiC [22], there seems to be no reasonable explanation for a smaller steady-state creep for composites than for monolithic SiC. Moreover, typically the chemically vapor-infiltrated SiC matrix is microstructurally more defected than monolithic CVD SiC in an as-grown condition. Therefore, the most likely cause is the smaller transient creep for the SiC fiber than CVD SiC. In the production process, TyrannoTM-SA fiber is final heat-treated at $\sim 1,800^\circ\text{C}$ under substantial tensile stress, which might have already modified the microstructural defects anisotropically so that the additional relaxation in favor of longitudinal tensile deformation is impeded. There has also been a proposed mechanism of grain boundary strengthening for TyrannoTM-SA fiber by nano-scopic precipitation of aluminum compound that obstructs high temperature deformation associated with grain boundary sliding and/or rearrangement [23], which may also affect the transient irradiation creep behavior. In either case, it is worth noting that the anticipated creep vulnerability of carbon interphase did not impose a detectable detrimental effect on irradiation creep of the composites.

Conclusions

Irradiation creep of vapor-deposited beta-phase SiC and uni-directional SiC composites were studied by BSR experiments in fission reactors. Irradiation creep strain for monolithic SiC exhibited weak temperature dependence in the $400\text{--}1,030^\circ\text{C}$ range. The creep strain appeared highly non-linear to neutron fluence due to the early domination of the initial transient irradiation creep. The transient creep was speculated to have caused by the rapid development of defect clusters and the structural relaxation of as-grown defects

during early stages of irradiation damage accumulation. Steady-state irradiation creep compliance of SiC was conservatively estimated to be $2\text{--}3 \times 10^{-32} \text{ (MPa}\cdot\text{n/m}^2\text{)}^{-1}$ at $\sim 600\text{--}\sim 1,100^\circ\text{C}$.

Both the monocrystalline beta-phase SiC and the uni-directionally reinforced Tyranno™-SA fiber, vapor-infiltrated SiC matrix composites exhibited substantially smaller creep strain than the polycrystalline beta-phase SiC at $0.2\text{--}0.74 \times 10^{24} \text{ n/m}^2$ and $600\text{--}1,030^\circ\text{C}$. These were attributed to differences in the transient irradiation creep strain, and several potential mechanisms were discussed.

References

- [1] Y. Katoh et al., Current Status and Critical Issues for Development of SiC Composites for Fusion Applications, *Journal of Nuclear Materials* (submitted).
- [2] S. J. Zinkle, *Fusion Sci. Technol.* 47 (2005) 821–828.
- [3] R. Naslain, *Compos. Sci. Technol.* 64 (2004) 155–170.
- [4] M. Abdou, D. Sze, C. Wong, M. Sawan, A. Ying, N. B. Morley, and S. Malang, *Fusion Sci. Technol.* 47 (2005) 475–487.
- [5] G. O. Hayner et al., INEEL/EXT-04-02347, Rev. 1, Idaho National Engineering and Environmental Laboratory, Idaho Falls (2004).
- [6] A. Kohyama, T. Hinoki, T. Mizuno, T. Kunugi, M. Sato, Y. Katoh, and J. S. Park, R&D of Advanced Material Systems for Reactor Core Component of Gas Cooled Fast Reactor, Proceedings of the International Congress on Advances in Nuclear Power Plants, May 15–19, 2005, Seoul.
- [7] A. R. Raffray, R. Jones, G. Aiello, M. Billone, L. Giancarli, H. Golfier, A. Hasegawa, Y. Katoh, A. Kohyama, S. Nishio, B. Riccardi, and M. S. Tillack, *Fusion Eng. Des.* 55 (2001) 55–95.
- [8] R. J. Price, *Nucl. Technol.* 35 (1977) 320–336.
- [9] R. Scholz, *J. Nucl. Mater.* 258–263 (1998) 1533–1539.
- [10] R. Scholz, *J. Nucl. Mater.* 254 (1998) 74–77.
- [11] R. Scholz and G. E. Youngblood, *J. Nucl. Mater.* 283–287 (2000) 372–375.
- [12] R. Scholz, R. Mueller, and D. Lesueur, *J. Nucl. Mater.* 307–311 (2002) 1183–1186.
- [13] J. A. DiCarlo, *J. Mater. Sci.* 21 (1986) 217–224.
- [14] G. N. Morscher and J. A. DiCarlo, *J. Am. Ceram. Soc.* 75 (1992) 136–140.
- [15] Y. Katoh and L. L. Snead, *Ceram. Eng. Sci. Proc.* 26, No. 2 (2005) 265–272.
- [16] Y. Katoh and L. L. Snead, *J. ASTM Int.* 2 (2005) 12377-1-13.
- [17] Y. Katoh, H. Kishimoto, and A. Kohyama, *J. Nucl. Mater.* 307–311 (2002) 1221–1226.
- [18] S. Kondo et al., *Journal of Nuclear Materials* (submitted).
- [19] Y. Katoh, N. Hashimoto, S. Kondo, L. L. Snead, and A. Kohyama, Microstructural Development in Cubic Silicon Carbide during Irradiation at Elevated Temperatures, *Journal of Nuclear Materials* (in press).
- [20] E. Polychroniadis, M. Syvajarvi, R. Yakimova, and J. Stoemenos, *J. Cryst. Growth* 263 (2004) 68–75.
- [21] G. N. Morscher, C. A. Lewinsohn, C. E. Bakis, R. E. Tressler, and T. Wagner, *J. Am. Ceram. Soc.* 78 (1995) 3244–3255.
- [22] T. D. Burchell, *Carbon Materials for Advanced Technologies*, Ed., T. D. Burchell (Pergamon, 1999).
- [23] T. Shibayama, private communication.